Comparison of breast density measured on MR images acquired using fat-suppressed versus nonfat-suppressed sequences[a)]

Daniel H.-E. Chang
Tu & Yuen Center for Functional Onco-Imaging and Department of Radiological Sciences, University of California, Irvine, California 92697

Jeon-Hor Chen[b)]
Tu & Yuen Center for Functional Onco-Imaging and Department of Radiological Sciences, University of California, Irvine, California 92697; Department of Radiology, China Medical University Hospital, Taichung 404, Taiwan; and Department of Medicine, College of Medicine, China Medical University, Taichung 404, Taiwan

Muqing Lin, Shadfar Bahri, and Hon J. Yu
Tu & Yuen Center for Functional Onco-Imaging and Department of Radiological Sciences, University of California, Irvine, California 92697

Rita S. Mehta
Department of Medicine, University of California, Irvine, California 92697

Ke Nie
Tu & Yuen Center for Functional Onco-Imaging and Department of Radiological Sciences, University of California, Irvine, California 92697

David J. B. Hsiang
Department of Surgery, University of California, Irvine, California 92697

Orhan Nalcioglu
Tu & Yuen Center for Functional Onco-Imaging and Department of Radiological Sciences, University of California, Irvine, California 92697 and Department of Cogno-Mechatronics Engineering, Pusan National University, Busandaehak-ro 63beon-gil, Geumjeong-gu, Busan 609-735, Korea

Min-Ying Su
Tu & Yuen Center for Functional Onco-Imaging and Department of Radiological Sciences, University of California, Irvine, California 92697

(Received 1 March 2011; revised 3 August 2011; accepted for publication 6 September 2011; published 17 October 2011)

Purpose: To investigate the difference of MR percent breast density measured from fat-suppressed versus nonfat-suppressed imaging sequences.
Methods: Breast magnetic resonance imaging (MRI) with and without fat suppression was acquired from 38 subjects. Breasts were divided into subgroups of different morphological patterns ("central" and "intermingled" types). Breast volume, fibroglandular tissue volume, and percent density were measured. The results were compared using nonparametric statistical tests and regarded as significant at $p < 0.05$.
Results: Breast volume, fibroglandular volume, and percent density between fat-suppressed and nonfat-suppressed sequences were highly correlated. Breast volumes measured on these two sequences were almost identical. Fibroglandular tissue volume and percent density, however, had small (<5%) yet significant differences between the two sequences—they were both higher on the fat-suppressed sequence. Intraobserver variability was within 4% for both sequences and different morphological types. The fibroglandular tissue volume measured on downsampled images showed a small (<5%) yet significant difference.
Conclusions: The measurement of breast density made on MRI acquired using fat-suppressed and nonfat-suppressed T1W images was about 5% difference, only slightly higher than the intraobserver variability of 3%–4%. When the density data from multiple centers were to be combined, evaluating the degree of difference is needed to take this difference into account. [DOI: 10.1118/1.3646756]

Key words: quantitative breast density, 3D breast parenchymal morphology, pulse sequence comparison, fat suppression

I. INTRODUCTION

Breast density refers to the amount of fibroglandular tissue as opposed to fatty tissue within the breast. It is commonly measured using mammography and referred to as "mammographic density." Extensive studies have shown that mammographic density is closely related to the occurrence of breast cancer.[1–4] Boyd *et al*. found a 2% increase in relative risk for breast cancer for every 1% increase in percent mammographic density (PMD), i.e., a woman with 50% PMD will have twice the cancer risk of a woman with entirely fatty breasts (0% PMD).[5] However, despite strong evidence and extensive report in the literature, mammographic density has not yet been used in the clinical setting for management of patients, which may be partly due to the difficulty in obtaining reliable measures. The evaluation of breast density based on mammography suffers from several major problems, including tissue-overlapping due to mammography's 2D image nature, variability in subject positioning and degree of compression/angle that leads to differing projection views, and variability in the x-ray intensity, detector setting, and calibration of mammography machines.[6]

In recent years, much effort has been made to develop more reliable quantitative methods for assessing breast density in order to better understand the link between breast density and cancer risk. Studies that measure breast density using images acquired by magnetic resonance imaging (MRI) have been reported.[7–16] MRI provides a noncompressed, three-dimensional view of breast tissue with strong soft tissue contrast between fibroglandular and fatty tissue; it also does not suffer from the issues of tissue overlap or x-ray exposure calibration present in mammography. The percent density is calculated as the ratio of fibroglandular tissue volume to total breast volume. This requires MR images with sufficiently high spatial resolution and clear tissue contrast to allow segmentation of the breast and fibroglandular tissue.

Although breast MRI is a widely used clinical imaging modality, the imaging protocols still vary from institution to institution.[17] Currently, there is no consensus in the breast MRI community as to which sequences should be included in a clinical protocol. The American College of Radiology (ACR) currently recommends the acquisition of high spatial resolution, fat-suppressed images. Directly evaluating postcontrast fat-suppressed images without using subtraction can avoid the problem of misregistration caused by the patient's motion during the acquisition of precontrast and postcontrast images.[18] On the other hand, the European Society of Breast Imaging (EUSOBI) currently recommends the use of subtraction images generated from nonfat-suppressed sequence over that of fat-suppressed images.[19] In general, compared to fat-suppressed images, nonfat-suppressed images show a higher signal-to-noise ratio and stronger tissue contrast. Among the several published studies measuring breast density using MRI, both fat-suppressed and nonfat-suppressed images have been used,[7–16] but comparison of the measured breast density based on these two sets of images has not been reported yet.

Previously, we have developed a quantitative method for measuring breast density based on nonfat-suppressed T1WI.[15] Since fat-suppressed and nonfat-suppressed sequences are both commonly used in current clinical breast MRI protocols, the purpose of this study was to compare the breast volume, fibroglandular tissue volume, and percent density measured from images of the same subjects acquired using these two sequences. Because the generated contrast between fibroglandular and fatty tissue is different, the impact on the reproducibility of the operator in density measurement was also studied. Furthermore, the morphological distribution pattern of the fibroglandular tissue can be categorized as a central pattern (densely packed fibroglandular tissue inside surrounded by fatty outside) or intermingled pattern (mixed fibroglandular and fatty tissues),[20] and how this pattern affects the density measurement was studied. In addition, the densities measured using images of different spatial resolutions were compared to investigate the impact of spatial resolution.

II. MATERIALS AND METHODS

II.A. Subjects and image acquisition

The study cohort consisted of 38 female subjects (age 28–82 years old, mean 48) who had a breast MRI performed between February 2008 and February 2009 at our research institution. All subjects had pathologically confirmed cancer in one breast, and a normal breast in the contralateral side without any lesion or prior procedures. Only the normal breast was analyzed in this work. All MRI studies were conducted with a 3.0T scanner (Philips, Best, The Netherlands). The fat-suppressed and nonfat-suppressed T1-weighted images used for analyzing breast density were acquired before contrast injection. The fat-suppressed imaging sequence was a 3D gradient echo with short TI inversion recovery (SPAIR) fat-suppression, with TR = 6.20 ms, TE = 1.26 ms, flip angle = 12°, matrix size = 480 × 480, FOV = 31–38 cm, slice thickness = 1 mm, and 160 axial slices. The nonfat-suppressed sequence was a 2D turbo spin-echo with TR = 800 ms, TE = 8.6 ms, flip angle = 90°, matrix size = 480 × 480, FOV = 31–38 cm, slice thickness = 2 mm, and 84 axial slices. This study was approved by the Institutional Review Board and was HIPAA-compliant. All subjects gave written informed consent.

II.B. MR-based breast density measurements

The breast volume and fibroglandular tissue volume were measured using a semiautomated MR-based method.[15] The percent density was calculated as the fibroglandular tissue volume divided by total breast volume. The key procedures included: (1) selecting the range of axial slices containing the breast; (2) using anatomic landmarks to define the lateral boundaries of the breast (Fig. 1, a horizontal truncation line was drawn through the point located 5 mm dorsal to the posterior margin of the sternum); (3) applying a fuzzy c-means (FCM) based segmentation algorithm with the b-spline curve fitting to obtain the breast boundary; (4) applying dynamic searching to exclude the skin along the breast boundary; (5)

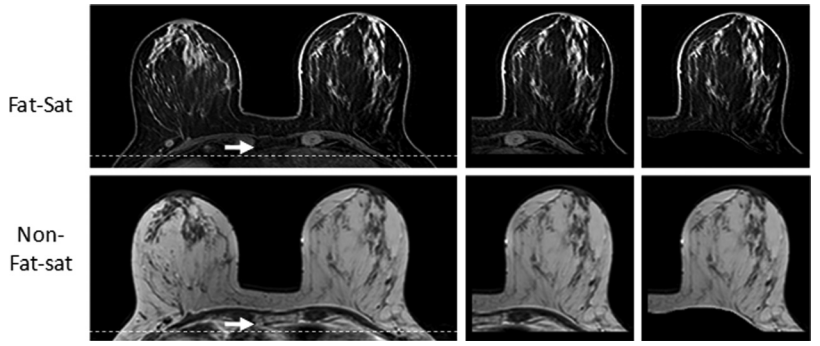

FIG. 1. Anatomical landmark on axial, precontrast fat-suppressed and nonfat-suppressed images. The fat-suppressed imaging sequence was a 3D gradient echo with SPAIR fat-suppression, with TR = 6.20 ms, TE = 1.26 ms, flip angle = 12°, matrix size = 480 × 480, FOV = 31–38 cm, slice thickness = 1 mm, and 160 axial slices. The nonfat-suppressed sequence was a 2D turbo spin-echo with TR = 800 ms, TE = 8.6 ms, flip angle = 90°, matrix size = 480 × 480, FOV = 31–38 cm, slice thickness = 2 mm, and 84 axial slices. The spatial location 5 mm posterior to the dorsal margin of the sternum, indicated by the arrow, is used as the point through which a horizontal line is drawn (a). The nonbreast tissue is excluded (b), resulting in defined breast tissue (c). The contrast between breast tissue and the pectoral muscle on both fat-suppressed and nonfat-suppressed images is very clear, showing reverse signal intensities, which allows a successful segmentation to remove the pectoral muscle on both sets of images.

applying bias field correction to remove image intensity nonuniformities; and (6) applying a fuzzy-c-means (FCM) clustering algorithm to segment fibroglandular tissue from fatty tissue in a slice by slice fashion. After the segmentation was completed, the breast volume, fibroglandular tissue volume and the percent density were calculated. The results analyzed based on fat-suppressed versus nonfat-suppressed images were compared.

II.C. Analysis of intraobserver reproducibility

The intraobserver reproducibility was evaluated by one operator on all 38 cases. The segmentation was done three times, with a minimum interval of 2 weeks between each analysis session. The coefficient of variation was used to indicate the reproducibility, which was calculated as the ratio of the standard deviation of three measurements done in three analysis sessions over their mean.

II.D. Impact of breast parenchymal pattern

To investigate how the morphological distribution pattern of the fibroglandular tissue (i.e., the parenchymal pattern) would affect the performance of segmentation and percent density quantification, the 38 breasts were further divided into two subtypes: central pattern (those showing densely packed fibroglandular tissue inside surrounded by fatty tissue outside, Fig. 2) and intermingled pattern (those showing intermingled fibroglandular and fatty tissues, Fig. 3). The categorization was performed by a radiologist and an experienced imaging scientist. They reached a consensus on the final categorization of 17 central patterns and 21 intermingled patterns. All density and reproducibility parameters within each pattern subgroup were also analyzed separately.

II.E. Impact of spatial resolution

In addition to performing segmentation on images at their original spatial resolution, segmentation was also done on images that had been downsampled to investigate the impact of differing resolutions on the measurements. This analysis was done in 23 randomly selected cases, 10 of the central pattern and 13 of the intermingled pattern. The in-plane spatial resolution in each dimension was decreased by a factor of 2 via bicubic interpolation—that is, the signal intensities of 4 pixels were averaged as the intensity of the new pixel to form a low resolution image. The low pass filtering was not performed prior to down-sampling. Breast volumes, fibroglandular tissue volumes, and percent density measured on these images were compared with those measured on the original images. There was no resolution reduction along the slice thickness direction and all imaging slices were analyzed.

II.F. Statistical analysis

Spearman's Rho was used to determine bivariate correlation between corresponding measurements from fat-suppressed and nonfat-suppressed images. Wilcoxon's

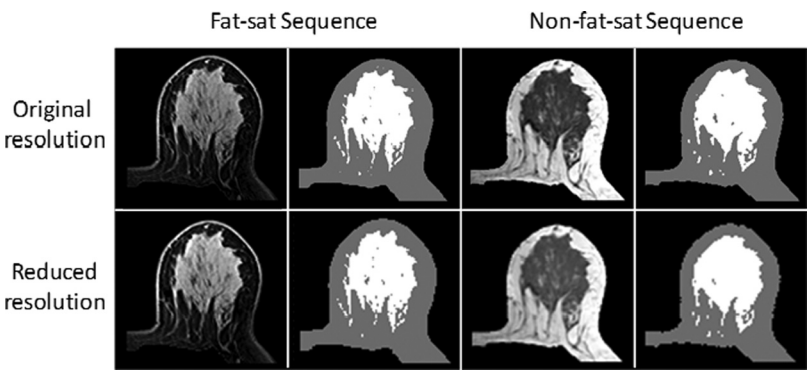

FIG. 2. An example of density segmentation on a "Central" type breast of a 39-year-old patient, showing confined fibroglandular tissue surrounded by fatty tissue. The contrast between fibroglandular tissue and fatty tissue is strong on both sets of images. On nonfat-suppressed images, the fibroglandular tissue is dark; on fat-suppressed images, the fibroglandular tissue is bright and nearly mirrored and reversed. Some subtle differences exist on the segmented fibroglandular tissues, but the quality is acceptable on both sets of images without obvious errors. Compared with the original image, the downsampled image is blurred, yet the contrast remains very strong for segmentation. The measurement results are listed in Table II.

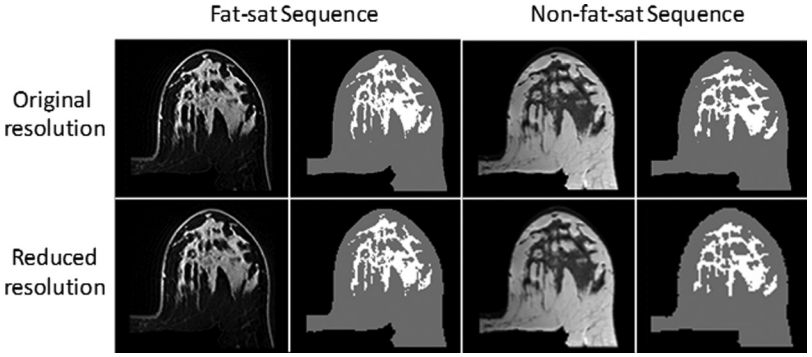

FIG. 3. An example of density segmentation on an "Intermingled" type breast of a 31-year-old patient, showing mixed fibroglandular tissue and fatty tissue. The segmented fibroglandular tissue region is slightly larger on fat-suppressed images. Nevertheless, the quality is acceptable on both sets of images without obvious errors. Compared with the original image, the downsampled image is blurred, yet the contrast remains very strong for segmentation, and the segmentation results are similar. The measurement results are listed in Table II.

signed ranks test (matched pairs test) was applied to determine the differences between measurements based on fat-suppressed versus nonfat-suppressed images and original versus reduced spatial resolution. All statistical tests were regarded as significant at $p < 0.05$.

III. RESULTS

III.A. Comparison of measurements between two sequences

The results of breast volume, fibroglandular tissue volume, and percent density measured on fat-suppressed and nonfat-suppressed images are listed in Table I. The original images and segmented density maps are shown in two examples, a central pattern case in Fig. 2 and an intermingled pattern case in Fig. 3. Figure 4 plots the volumes and percent density measured on the fat-suppressed sequence versus the nonfat-suppressed sequence. They were all highly correlated with $p < 0.001$ using Spearman's Rho.

The correlation slope was 1.0019 for breast volume, indicating that the volumes measured on these two sequences were almost identical. In the whole group of 38 breasts, the breast volume was 681 ± 359 (mean $\pm$ stdev) cm^3 on fat-suppressed sequence and 679 ± 361 cm^3 on nonfat-suppressed sequence, which was not significantly different as determined by the Wilcoxon's signed ranks test. For fibroglandular tissue volume and percent density, although there was a high correlation, a slope greater than 1.0 suggested that the values measured from fat-suppressed images were greater than those from nonfat-suppressed images. The fibroglandular tissue volume was 100 ± 58 cm^3 on fat-suppressed images, which was slightly higher than 97 ± 58 cm^3 on nonfat-suppressed images. The difference was significant with $p < 0.003$ using the Wilcoxon's signed ranks test. The percent density was $17.5\% \pm 9.5\%$ on fat-suppressed images, which was slightly higher than $17.0\% \pm 9.3\%$ on nonfat-suppressed images, also significant with $p < 0.032$. The relatively high standard deviation was common, which indicated the high individual variability among the 38 patients. Comparison of the parameters measured on fat-suppressed and nonfat-suppressed sequences used matched pairs, and only the values measured from the same woman were being compared.

III.B. Comparison in central versus intermingled subtypes

The analysis was also performed separately in the central pattern (N = 17) and intermingled pattern (N = 21) subtypes.

TABLE I. Breast volume, fibroglandular tissue volume and percent density measured on fat-suppressed and nonfat-suppressed images in different groups.

		Breast type subgroups: Nonfat-suppressed versus Fat-suppressed						
		Fat-sup	Nonfat-sup	Difference	Wilcoxon[a]	Spearman's[b]	Intraobserver[c]	
		(mean ± stdev)	(mean ± stdev)	(mean ± stdev)	Signed Ranks	Rho	fatsup	nonfatsup (%)
Entire group N = 38	**BV (cm^3)**	681 ± 359	679 ± 361	7.7 ± 4.9	$p < 0.212$	0.999	2.70	3.33
	FV (cm^3)	100 ± 58	97 ± 58	5.0 ± 3.2	**$p < 0.003$**	0.997	2.48	3.10
	PD (%)	17.5% ± 9.5%	17.0% ± 9.3%	0.8% ± 0.6%	**$p < 0.032$**	0.970	2.85	2.71
Central type N = 17	**BV (cm^3)**	485 ± 259	482 ± 259	7.1 ± 5.2	$p < 0.386$	0.999	2.70	3.39
	FV (cm^3)	97 ± 61	94 ± 62	5.5 ± 2.9	$p < 0.139$	0.999	3.06	3.40
	PD (%)	20.3% ± 8.2%	20.0% ± 8.1%	1.0% ± 0.6%	$p < 0.285$	0.952	3.17	1.69
Intermingled type N = 21	**BV (cm^3)**	832 ± 359	830 ± 362	8.1 ± 4.8	$p < 0.422$	0.999	2.69	3.27
	FV (cm^3)	102 ± 59	98 ± 57	4.6 ± 3.5	**$p < 0.011$**	0.995	1.81	2.75
	PD (%)	15.2% ± 10.2%	14.7% ± 9.9%	0.7% ± 0.5%	**$p < 0.033$**	0.989	2.47	3.89

[a]Significant difference between measurements made on fat-suppressed and nonfat-suppressed images is determined using the Wilcoxon signed ranks (matched pair) test.
[b]The correlation from all subjects in each group is assessed using the Spearman's rho test.
[c]Intraobserver reproducibility is expressed as averaged coefficient of variation (standard deviation from three separate measurements over the mean) from all subjects in each group.

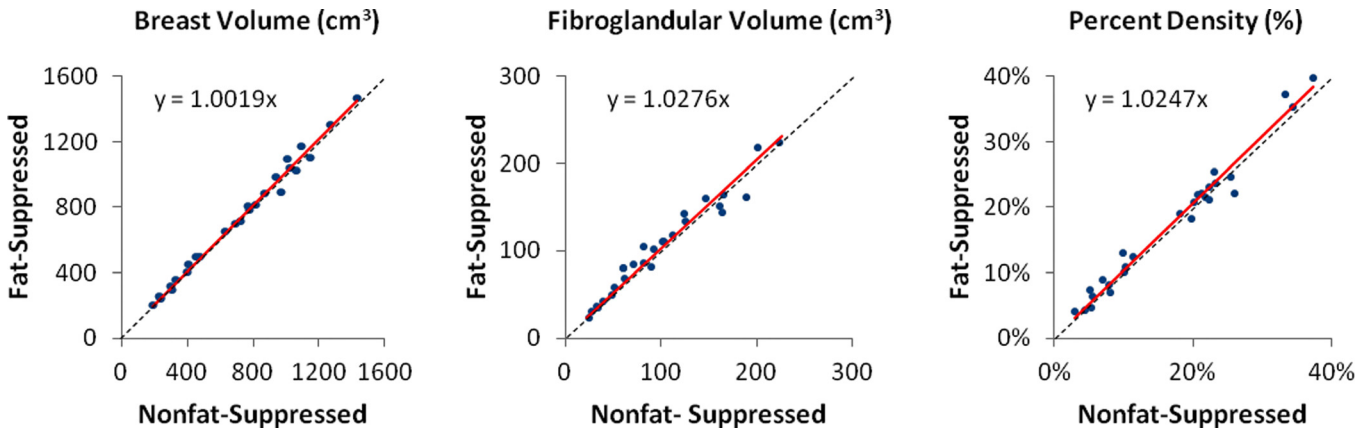

FIG. 4. Spearman's Rho between measurements from fat-suppressed and nonfat-suppressed images for (a) breast volume, (b) fibroglandular tissue volume, and (c) percent density. The parameters measured from the fat-suppressed sequence are on the y-axis; from the nonfat-suppressed sequence are on the x-axis. They are highly correlated with $p < 0.001$. The best-fit line passing through the origin is plotted on the figure, with a slope of 1.0019 for breast volume, 1.0276 for fibroglandular tissue volume, and 1.0247 for percent density. The dotted black line indicates the unity line representing 1:1 correlation. The least squares regression line lies close to the unity line.

In the central subtype, although the mean values were higher on fat-suppressed than on nonfat-suppressed images, the differences in breast volume (485 ± 259 cm^3 on fat-suppressed, 482 ± 259 cm^3 on nonfat-suppressed, $p < 0.386$), fibroglandular tissue volume (97 ± 61 cm^3 on fat-suppressed, 94 ± 62 cm^3 on nonfat-suppressed, $p < 0.139$), and percent density ($20.3\% \pm 8.2\%$ on fat-suppressed, $20.0\% \pm 8.1\%$ on nonfat-suppressed, $p < 0.285$), were not significant. In the intermingled subtype, the difference in breast volume (832 ± 359 cm^3 on fat-suppressed, 830 ± 362 cm^3 on nonfat-suppressed, $p < 0.422$) was not significant. But the differences in fibroglandular tissue volume (102 ± 59 cm^3 on fat-suppressed, 98 ± 57 cm^3 on nonfat- suppressed, $p < 0.011$) and percent density ($15.2\% \pm 10.2\%$ on fat-suppressed, $14.7\% \pm 9.9\%$ on nonfat-suppressed, $p < 0.033$) were significant—higher on fat-suppressed than on nonfat- suppressed images.

III.C. Intraobserver reproducibility

The intraobserver reproducibility was determined by analyzing all 38 cases 3 times. The coefficients of variation analyzed on fat-suppressed and nonfat-suppressed images in the whole group, as well as in the separated central and intermingled pattern subtypes, are listed in Table I. The coefficient of variation was between 1.5% and 4.0% for all measures, which was similar to the range of previously reported reproducibility for MRI-based density measurements [15]. There was no obvious difference in the range of reproducibility between the fat-suppressed versus nonfat-suppressed sequences, or between the central versus intermingled patterns.

III.D. Impact of different spatial resolution

The downsampled images and segmented density maps are also shown in Figs. 2 and 3. The segmentation results for these two cases are listed in Table II. The measured breast volumes on both fat-suppressed and nonfat-suppressed images were increased slightly on the downsampled images compared with original images, by 0.5%–1.5%. For central pattern cases (Fig. 2), the fibroglandular tissue volume on downsampled images was decreased by 4% on both fat-suppressed and nonfat-suppressed images. For intermingled pattern cases (Fig. 3), the fibroglandular tissue volume on downsampled images was decreased by 4% on fat-suppressed images but was much higher by 8% on the nonfat-suppressed image [which is clearly visible comparing Figs. 3(f) with Fig. 3(b)]. Due to the increased fibroglandular tissue volume and slightly decreased breast volume, the percent density was also increased on downsampled images.

TABLE II. Parameters measured on images at original and reduced spatial resolution for cases shown in Figs. 2 and 3.

Downsampling by a factor of 2: Fat-suppressed versus nonfat-suppressed							
		Fat-suppressed			Nonfat-suppressed		
		Original	Reduced	Diff (%)	Original	Reduced	Diff (%)
Central type (Fig. 2)	**Breast volume (cm^3)**	714	725	1.4	725	736	1.5
	Fibro volume (cm^3)	152	146	3.7	162	155	3.8
	Percent density (%)	21.2%	20.2%	4.7	22.3%	21.1%	5.4
Intermingled type (Fig. 3)	**Breast volume (cm^3)**	914	924	1.1	910	915	0.6
	Fibro volume (cm^3)	140	134	4.3	141	130	8.0
	Percent density (%)	15.4%	14.6%	5.2	15.5%	14.2%	8.4

TABLE III. Parameters measured on images at original and reduced spatial resolution.

Downsampling by a factor of 2: Fat-suppressed versus nonfat-suppressed							
		Fat-suppressed			Nonfat-suppressed		
		Original (mean ± stdev)	Reduced (mean ± stdev)	Wilcoxon Signed ranks	Original (mean ± stdev)	Reduced (mean ± stdev)	Wilcoxon Signed ranks
Central type (N = 10)	**Breast volume (cm^3)**	485 ± 259	496 ± 261	$p < 0.022$	482 ± 259	494 ± 260	$p < 0.018$
	Fibro volume (cm^3)	97 ± 61	93 ± 60	$p < 0.005$	94 ± 62	89 ± 60	$p < 0.007$
	Percent density (%)	20.3% ± 8.2%	18.8% ± 7.9%	$p < 0.007$	20.0% ± 8.1%	18.9% ± 8.0%	$p < 0.009$
Intermingled type (N = 13)	**Breast volume (cm^3)**	832 ± 359	842 ± 363	$p < 0.031$	832 ± 362	843 ± 363	$p < 0.024$
	Fibro volume (cm^3)	102 ± 59	97 ± 58	$p < 0.017$	98 ± 57	92 ± 58	$p < 0.009$
	Percent density (%)	15.2% ± 10.2%	14.1% ± 9.8%	$p < 0.012$	14.7% ± 9.9%	13.4% ± 9.8%	$p < 0.010$

Among all 23 analyzed cases (10 with central pattern and 13 with intermingled pattern), the measured breast volume, fibroglandular tissue volume, and percent density based on original images and on downsampled images are summarized in Table III. Breast volume measured on both fat-suppressed and nonfat-suppressed images was slightly higher than that of the original images (in the vicinity of 2%), while fibroglandular volume on both sequences was lower than that of the original images (in the vicinity of 5%). As a result of decreased fibroglandular volume and increased breast volume, the percent density was decreased on the downsampled images (in the vicinity of 7%). The Wilcoxon's signed ranks test based on matched pairs found that the differences in breast volume, fibroglandular volume, and breast density between original and downsampled images were all significant. The difference most likely came from the increased partial volume effect with decreased spatial resolution.

IV. DISCUSSION

The Breast Cancer Prevention Collaborative Group (BCPCG) has recommended that breast density should be incorporated into the risk prediction model to improve its accuracy.[21] So far, none of the established cancer risk prediction models (e.g., Gail, Claus, BRACPRO, Cuzik-Tyrer) takes breast density into account. MRI-based breast density may provide more detailed volumetric and morphological parameters compared to mammography and will be able to contribute unique information. To develop a new risk prediction model, a large dataset is needed. Since many women are receiving screening MRI, they can be used as a large cohort to build a model incorporating MRI-based density, but the ability to analyze and combine data from multiple institutions is essential for the success.

Of the eight studies that we found reporting quantitative analysis of breast density on MRI, four studies used nonfat-suppressed images;[8,10,11,16] while the other four[7,12–14] used fat-suppressed images. In several previous publications, we analyzed breast density on nonfat-suppressed images.[15,20,22–25] The purpose of the present study is to address the current lack of published studies investigating the difference in breast density measured using fat-suppressed versus nonfat-suppressed sequences. Our breast MRI protocol follows the ACR recommendation and uses fat-suppressed sequence for the dynamic contrast enhanced study. For performing this study, a nonfat-suppressed sequence was added before contrast injection, so the density parameters measured using these two sequences could be compared.

As the 3D MRI quantification of breast density depends on segmentation of fibroglandular tissue, the imaging quality and tissue contrast of different pulse sequences may impact the performance of computer-based algorithms and thereby the segmentation results. Breast MRI is acquired using the surface breast coil to cover a large region with a large field of view, and inevitably the signal intensity may vary depending on the location of the tissue.[17,26] The different degrees of inhomogeneity on fat-suppressed and nonfat-suppressed images may affect the segmentation and quantification of density parameters.

The measurement of breast volume on fat-suppressed and nonfat-suppressed sequences was highly correlated. In fact, the correlation was 1:1. This correlation was true for the entire cohort, including both central and intermingled patterns. The major variations for the segmentation of breast from the body came from the placement of the initial cut-line, as well as the contrast between the breast tissue and the pectoral muscle for the b-spline fitting to find the posterior breast boundary.[15] In this study, the truncation line was chosen based on the point located 5 mm dorsal to the posterior margin of the sternum. As shown in Fig. 1, this landmark is clearly visible on both fat-suppressed and nonfat-suppressed images, and not a source of variation between these two sequences. One note that we need to point out is that the skin is much more visible on fat-suppressed images than on nonfat-suppressed images; however, skin was counted as part of the breast volume for all statistical and correlation analyses done in this work, and it is not a source of variation in the presented breast volume measurements.

For fibroglandular tissue volume and percent density, there was a statistically significant difference showing slightly higher values on fat-suppressed images compared with nonfat-suppressed images despite the high correlation between results analyzed from fat-suppressed and nonfat-suppressed images. The analyses based on different density morphology patterns showed a significant difference in the intermingled pattern but not in the central pattern (will reach 80% power when the subject number increases from 17

to 37). The results suggest that the performance of the FCM-based segmentation method is affected by breast morphology. The problem of partial volume effect (a pixel containing both fibroglandular tissue and fatty tissue) is more severe for the intermingled pattern cases than the central pattern cases, which may have contributed to the difference.

As shown in Table I, the mean difference in the fibroglandular tissue volume analyzed on fat-suppressed versus nonfat-suppressed sequences was in the order of 5 cm^3, which was approximately 5% higher (over the mean fibroglandular tissue volume of 100 cm^3). For percent density, the difference was also 5% higher (0.8% difference over the mean of 17%). We have tried to investigate whether there was a systematic difference. The segmentation results based on fat-suppressed and nonfat-suppressed images were placed side-by-side, and scrolled through slice-by-slice for inspection, but revealed no definitive explanation for the underlying differences. The 5% difference is very small, and a subtle difference on several slices can easily add up to a 5% difference. Since the imaging parameters for fat-suppressed and nonfat-suppressed sequences cannot be made exactly identical, direct comparison based on superimposing the segmentation results to definitively identify differences is not feasible.

The intraobserver reproducibility was analyzed in all 38 cases. The coefficient of variation obtained from three separate analysis sessions was in the range of 3% for all 38 subjects. Within the central pattern subtype or intermingled pattern subtype, the coefficient of variation for each measured parameter may be higher or lower, but also in the vicinity of 3%. The source of variation for breast volume segmentation has been described earlier. For the segmentation of fibroglandular tissue using the FCM algorithm, it is known that the major source of variation comes from the number of FCM clusters used by the operator. In the present study, a total of six clusters was used, three for fibroglandular, and three for fatty tissues. Fixing the number of clusters helped to keep the intraobserver variation of the fibroglandular tissue and the percent density close to 3%, which was similar to the variation for the breast volume. Given that the intraobserver variation was within 3%–4%, the 5% difference in the density parameters measured on fat-suppressed versus nonfat-suppressed sequences was only slightly higher than the intraobserver uncertainty.

The comparison of segmentation results based on the original and downsampled images revealed a small yet significant difference in breast volume, fibroglandular volume, and breast density. On the downsampled low spatial resolution images, breast volume was increased by 2%, and fibroglandular volume was decreased by 5%. Although the matched pair analysis showed that the difference was significant, visual inspection by scrolling through all slices cannot pick up this subtle difference (as the examples shown in Figs. 2 and 3). The difference may be explained by the partial volume effect. During downsampling, the air adjacent to the breast-air boundary was averaged in and becomes part of a breast pixel, and that increased the measured breast volume. In a similar but reversed way, fibroglandular tissue located near the fibroglandular-fat boundary had its intensity modified during the downsampling and subsequently became categorized by FCM as fat, which may have led to decreased fibroglandular tissue volume. However, since we could not find a systematic difference during visual inspection, the 5% difference could easily come from differences in a small region on several imaging slices.

In this study, the two imaging techniques, 2D spin-echo versus 3D gradient echo, compared were quite different, beyond just fat-suppression. The slice thicknesses were also different. Even though our study has found that the measurement of breast density made on MRI acquired using fat-suppressed and nonfat-suppressed T1W images was small (about 5% difference), it must be acknowledged that the findings were specific to the type of MRI approaches described in this study and may not be widely applicable without further investigation. In particular, the effect of image artifacts (e.g., signal heterogeneity) due to the different surface RF coils used in different medical institutions may potentially be one of the major sources of measurement variation for breast density. Also, the type of fat suppression used in this study was based on short TI inversion recovery (SPAIR), which is only one of the several approaches, including spectrally selective saturation pulses which would be expected to change the results somewhat, especially with varying shimming. The sample size used in this study was 38 cases, and further investigation in a larger cohort is required before any conclusion can be made about the way to use the density parameters measured on fat-suppressed and nonfat-suppressed imaging sequences interchangeably. Given that there was no systematic difference that could explain the observed difference between fat-suppressed and nonfat-suppressed images, or between images of different spatial resolutions, it is premature to recommend a correction factor. Furthermore, we have demonstrated that the difference may depend on the fibroglandular tissue distribution pattern and vary from case to case. It would be informative to conduct a larger study and determine whether the difference is also found in other experimental settings and thus can be generalized or is specific and applicable only to images analyzed in our study.

In summary, we have conducted a thorough study to compare the measurement of breast volume, fibroglandular tissue volume, and percent density based on fat-suppressed and nonfat-suppressed images of the same women. The measurement of breast density made using fat-suppressed and nonfat-suppressed T1W images had about a 5% difference, only slightly higher than the intraobserver variability of 3%–4%. For the future goal of developing an improved cancer risk prediction model by incorporating breast density, a larger database is needed. This can only be achieved with data from multiple sites after taking into account the impact of pulse sequences and acquisition parameters on the measured breast density. The work presented in this study is essential for integrating the breast densities analyzed from multiple institutions using fat-suppressed and nonfat-

suppressed sequences with different spatial resolutions for combined analysis.

ACKNOWLEDGMENT

This work was supported in part by NIH R01 CA127927, R03 CA136071, California BCRP #14GB-0148, #16GB-0056.

[a)]This study was conducted at Center for Functional Onco-Imaging, School of Medicine, University of California Irvine
[b)]Author to whom correspondence should be addressed. Electronic mail: jeonhc@uci.edu: Telephone: (949) 824-9327

[1]N. F. Boyd *et al.*, "Mammographic density and the risk and detection of breast cancer," N. Engl. J. Med. **356**, 227–236 (2007).
[2]V. A. McCormack and I. dos Santos Silva, "Breast density and parenchymal patterns as markers of breast cancer risk: A meta-analysis," Cancer Epidemiol. Biomarkers Prev. **15**, 1159–1169 (2006).
[3]C. M. Vachon *et al.*, "Longitudinal trends in mammographic percent density and breast cancer risk," Cancer Epidemiol. Biomarkers Prev. **16**, 921–928 (2007).
[4]N. F. Boyd, G. S. Dite, J. Stone, A. Gunasekara, D. R. English, M. R. McCredie, G. G. Giles, D. Tritchler, A. Chiarelli, M. J. Yaffe, and J. L. Hopper, "Heritability of mammographic density, a risk factor for breast cancer," N. Engl. J. Med. **347**, 886–894 (2002).
[5]N. F. Boyd, J. W. Byng, R. A. Jong, E. K. Fishell, L. E. Little, A. B. Miller, G. A. Lockwood, D. L. Tritchler, and M. J. Yaffe, "Quantitative classification of mammographic densities and breast cancer risk: Results from the Canadian National Breast Screening Study," J. Natl. Cancer Inst. **87**, 670–675 (1995).
[6]J. A. Harvey and V. E. Bovbjerg, "Quantitative assessment of mammographic breast density: Relationship with breast cancer risk," Radiology **230**, 29–41 (2004).
[7]J. Eng-Wong *et al.*, "Effect of Raloxifene on mammographic density and breast magnetic resonance imaging in premenopausal women at increased risk for breast cancer," Cancer Epidemiol. Biomarkers Prev. **17**, 1696–1701 (2008).
[8]M. Khazen *et al.*, "A pilot study of compositional analysis of the breast and estimation of breast mammographic density using three-dimensional T1-weighted magnetic resonance imaging," Cancer Epidemiol. Biomarkers Prev. **17**, 2268–2274 (2008).
[9]J. Wei *et al.*, "Correlation between mammographic density and volumetric fibroglandular tissue estimated on breast MR images," Med. Phys. **31**, 923–942 (2004).
[10]S. van Engeland, P. R. Snoeren, H. Huisman, C. Boetes, and N. Karssemeijer, "Volumetric breast density estimation from full-field digital mammograms," IEEE Trans. Med. Imaging **25**, 273–282 (2006).
[11]N. A. Lee *et al.*, "Fatty and fibroglandular tissue volumes in the breasts of women 20-83 years old: Comparison of x-ray mammography and computer-assisted MR imaging," AJR, Am. J. Roentgenol. **168**, 501–506 (1997).
[12]J. Yao, J. A. Zujewski, J. Orzano, S. Prindiville, and C. Chow, "Classification and calculation of breast fibroglandular tissue volume on SPGR fat suppressed MRI," Med. Image Proc. SPIE 1942–1949 (2005).
[13]C. Klifa *et al.*, "Quantification of breast tissue index from MR data using fuzzy cluster," Proc. IEEE Eng. Med. Biol. Soc. **3**, 1667–1670 (2004).
[14]C. Klifa *et al.*, "Magnetic resonance imaging for secondary assessment of breast density in a high-risk cohort," Magn. Reson. Imaging **28**, 8–15 (2010).
[15]K. Nie, J. H. Chen, S. Chan, M. K. Chau, H. J. Yu, S. Bahri, T. Tseng, O. Nalcioglu, and M. Y. Su, "Development of a quantitative method for analysis of breast density based on 3-dimensional breast MRI," Med. Phys. **35**, 5253–5262 (2008).
[16]D. J. Thompson *et al.*, "Assessing the usefulness of a novel MRI-based breast density estimation algorithm in a cohort of women at high genetic risk of breast cancer: The UK MARIBS study," Breast Cancer Res. **11**, R80 (2009).
[17]J. A. Harvey, R. E. Hendrick, J. M. Coll, B. T. Nicholson, B. T. Burkholder, and M. A. Cohen, "Breast MR imaging artifacts: How to recognize and fix them," Radiographics **27**(Suppl 1), S131–S145 (2007).
[18]E. A. Morris, "ACR practice guideline for the performance of contrast-enhanced magnetic resonance imaging (MRI) of the breast," Res. 25-2008. http://www.acr.org/SecondaryMainMenuCategories/quality_safety/guidelines/breast/mri_breast.aspx. Last accessed May 5, 2010.
[19]R. M. Mann, C. K. Kuhl, K. Kinkel, and C. Boetes, "Breast MRI: Guidelines from the European Society of Breast Imaging," Eur. Radiol. **18**, 1307–1318 (2008).
[20]K. Nie, D. Chang, J. H. Chen, C. C. Hsu, O. Nalcioglu, M. Y. Su, "Quantitative analysis of breast parenchymal patterns using 3D fibroglandular tissues segmented based on MRI," Med. Phys. **37**, 217–226 (2010).
[21]R. J. Santen, N. F. Boyd, R. T. Chlebowski, S. Cummings, J. Cuzick, M. Dowsett, D. Easton, J. F. Forbes, T. Key, S. E. Hankinson, A. Howell, and J. Ingle "Breast Cancer Prevention Collaborative Group. Critical assessment of new risk factors for breast cancer: Considerations for development of an improved risk prediction model," Endocr. Relat. Cancer **14**, 169–187 (2007).
[22]K. Nie, D. Chang, J. H. Chen, T. C. Shih, C. C. Hsu, O. Nalcioglu, and M. Y. Su, "Impact of skin removal on quantitative measurement of breast density using MRI," Med. Phys. **37**, 227–233 (2010).
[23]J. H. Chen, K. Nie, S. Bahri, C. C. Hsu, F. T. Hsu, H. N. Shih, M. Lin, O. Nalcioglu, and M. Y. Su, "Decrease in breast density in the contralateral normal breast of patients receiving neoadjuvant chemotherapy: MR imaging evaluation," Radiology **255**, 44–52 (2010).
[24]K. Nie, M. Y. Su, M. K. Chau, S. Chan, H. Nguyen, T. Tseng, Y. Huang, C. E. McLaren, O. Nalcioglu, and J. H. Chen, "Age- and race-dependence of the fibroglandular breast density analyzed on 3D MRI," Med. Phys. **37**, 2770–2776 (2010).
[25]J. H. Chen, Y. C. Chang, D. Chang, Y. T. Wang, K. Nie, R. F. Chang, O. Nalcioglu, C. S. Huang, and M. Y. Su, "Reduction of breast density following tamoxifen treatment evaluated by 3-D MRI: Preliminary study," Magn. Reson. Imaging **29**, 91–98 (2011).
[26]J. H. Chen, H. C. Le, J. A. Koutcher, and S. Singer, "Fat-free MRI based on magnetization exchange," Magn. Reson. Med. **63**, 713–718 (2010).